Oxidative Destruction of DNA by the Adriamycin–Iron Complex†

Helen Eliot, Luca Gianni,‡ and Charles Myers*

ABSTRACT: The 2:1 adriamycin–Fe(III) complex is able to bind to DNA and to catalyze its oxidative destruction. The binding of the drug–metal complex to DNA is indicated by characterstic spectral changes which are different from those seen with adriamycin intercalation and by the propensity of the drug–metal complex to precipitate DNA. Furthermore, intercalated adriamycin appears not to be available for iron binding. The resulting ternary complex is quite stable: it is not disrupted by incubation in the presence of EDTA and can be isolated by using Sephadex G-50 column chromatography. Disruption of the ternary complex requires vigorous conditions (extraction with phenol at 60 °C). The adriamycin–iron complex in free solution has the capacity to catalyze the reduction of oxygen by thiols. The DNA-bound drug–metal complex preserves this capacity over a wide range of complex/DNA ratios. As a consequence of this thiol-dependent oxygen reduction, DNA is cleaved. This thiol-dependent DNA cleavage has been shown to require hydrogen peroxide as an intermediate product. These results have led us to propose that the thiol-dependent DNA cleavage reaction has two stages involving (1) reduction of oxygen leading to hydrogen peroxide and then (2) peroxide-dependent DNA cleavage. An unusual property of this reaction is that the cleavage is not random but gives rise to a defined 2300 base pair fragment.

In an earlier paper, we reported that adriamycin formed a complex with Fe(III) and that the resulting metal ion complex bound to erythrocyte ghost membranes and, once bound, was able to catalyze the oxidative destruction of the erythrocyte ghost membrane (Myers et al., 1982). This oxidative destruction was unusual in that it resulted from thiol-dependent reduction of oxygen to superoxide and hydrogen peroxide by the membrane-bound drug–metal complex. In the present paper, we have extended these observations to the interaction between the adriamycin–Fe(III) chelate and DNA. This work was triggered by several observations. First, there is much literature on the binding of the adriamycin–Cu(II) complex to DNA (Fisherman & Schwartz, 1974; Mikelens & Levinson, 1978; Phillips & Carlyle, 1981; Spinelli & Dabrowiak, 1982; Fritzsche et al., 1982). Second, one of the most common histochemical techniques for staining DNA involves the use of the mordant dye technique in which Fe(III) or Al(III) acts as a bridge to link the dye to DNA (Lillie & Fallmer, 1976). Many of the dyes used in this technique are hydroxyquinone dyes (Figure 1) with structural similarities to adriamycin. Thus, iron-mediated binding seems feasible in that it appears to be a general property of hydroxyquinones of diverse structure. Third, Someya et al. (Someya & Tanaka, 1979) have recently reported that addition of adriamycin, a reducing agent, and Fe(III) or Cu(II) to DNA results in DNA cleavage. The results suggest that adriamycin–Fe(III) chelates might first bind to DNA and then cleave it via a chemistry similar to that observed in our study of erythrocyte ghost destruction. This paper investigates that hypothesis.

Materials and Methods

Adriamycin hydrochloride was provided by the Drug Synthesis and Chemistry Branch of the National Cancer Institute. ^{3}H SV-40 DNA, component I (strain 776), and the molecular weight standards ϕX174 FR DNA *Hae*III fragments and the phage λ DNA *Hin*dIII fragments were all purchased from Bethesda Research Laboratories, Inc., Gaithersburg, MD, and kept frozen at −20 °C until used. Ultra-Pure sucrose and agarose gel, electrophoresis grade, both negative for DNase and RNase activity, also were obtained from Bethesda Research Laboratories, Inc. Bovine superoxide dismutase, bovine liver catalase crystallized twice and containing 30 000–40 000 units/mg of protein, dimethyl sulfoxide, and L-histidine were all purchased from Sigma Chemical Co., St. Louis, MO. All other chemicals were reagent grade or better. Glass distilled water was used throughout the experiments.

Absorbance spectra were measured on the Hewlett-Packard 8540A diode array spectrophotometer which can be programmed to average the results of 25 scans.

The 2:1 adriamycin–Fe(III) complex was formed from the acetohydroxamic acid complex as previously described and used as such in all of the studies to be presented. Oxygen consumption studies were done as previously described (Myers et al., 1982).

Purification of the DNA. Two reagent solutions were required. SEVAG was composed of 1 volume of chloroform and $^1/_{24}$ volume of isoamyl alcohol. PC9 was composed of 0.5 volume of crystallized phenol, saturated with 50 mM Tris,[1] pH 9, and 0.5 volume of SEVAG. *Escherichia coli* DNA (65.6 mg) was dissolved in 10 mL of double-distilled water and brought to 0.2 M NaCl. This was divided evenly into two stoppered tubes and 1 volume of PC9 added to each, vortexed thoroughly, and spun at 10 000 rpm for 10 min at 4 °C in a Sorvall RC-5 centrifuge. The aqueous phase was saved and the extraction with PC9 repeated. One volume of SEVAG was added to the supernatants. After mixing, these were spun for 30 min at 10 000 rpm and 4 °C. The DNA was precipitated with 2 volumes of cold absolute ethanol, collected on a spool, and dried in a vacuum centrifuge (Savant SVC 100H speed vac concentrator, Savant Instrument, Inc., Hicksville, NY). It was then redissolved in 30 mL of double-distilled water.

Reaction of Complex with DNA. In these reactions, supercoiled SV40 DNA was used as a target for the adriamycin–iron complex. It is important to note that the drug–metal

† From the Clinical Pharmacology Branch, Division of Cancer Treatment, National Cancer Institute, Bethesda, Maryland 20205. *Received July 22, 1983.*

‡ Present address: Istituto Nazionale Tumori, Via Venezian 1, Milan, Italy.

[1] Abbreviations: Tris, tris(hydroxymethyl)aminomethane; GSH, reduced glutathione; EDTA, ethylenediaminetetraacetic acid; Me_2SO, dimethyl sulfoxide.

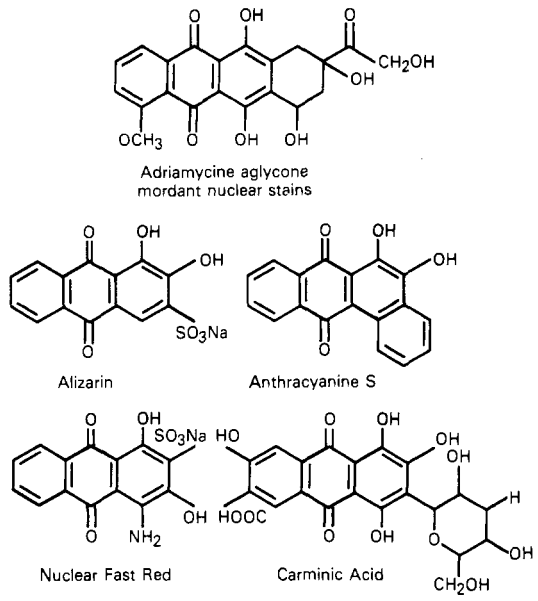

FIGURE 1: Structural similarities between adriamycin and several mordant nuclear strains.

complex engages in photochemistry which leads to dramatic DNA cleavage and, therefore, all reagents must be kept in the dark. Details of this photochemistry will be reported elsewhere.

For gradients, the standard reaction mixture contained 0.5 nmol of DNA and 2.5 nmol of ferric iron complexed by 5 nmol of adriamycin in a total volume of 50 μL. This mixture was incubated in the dark at room temperature for 2 h and then 40 μL of this placed on a 4.4-mL, 5–20% alkaline sucrose density gradient, containing 0.3 M NaOH and 0.9 M NaCl. The gradients were formed on a Beckman density gradient formed in cellulose nitrate tubes. Thirty 0.15-mL fractions were taken from the bottom of each tube. In most of our preparations there existed some form II, or relaxed double-standed circular DNA, due to a small proportion of single-stranded breaks. We were interested in any increase in the number of single-stranded or double-stranded breaks, giving either open linear pieces of DNA or relaxed circles. After a few preliminary centrifugations, in a Beckman 60 Ti swinging-bucket rotor, at various combinations of rpm and length of spin, we settled on the shortest spin time that would give us a good separation of fragmented from intact DNA with no overlapping of the curves. Excellent separation was obtained at 190000*g* for 135 to 150 min, with the supercoiled DNA rather uniformly peaking at fractions 5–7 and the fragmented DNA at 19–21. In each peak, dpm values above background were totaled, and the sum of the fragment dpm was divided by the dpm in the fractions containing intact DNA. The results were expressed as the fragmentation ratio. Controls of untreated DNA were always included for comparison.

For the agarose gels, the standard reaction mixture contained 24 nmol of DNA, 24 nmol of H_2O_2 or 60 nmol of GSH, and 12 nmol of ferric iron complexed by 24 nmol of adriamycin. The final volume was 240 μL, a sufficient volume for phenol extraction (see below). The agarose gels were run on an LKB 2001 vertical slab gel electrophoresis apparatus using a 2500-V power supply. The gels were 1% agarose, 3 mm thick, and were run in 40 mM Tris (pH 7.8) containing 5 mM sodium acetate and 1 mM EDTA. Gels were run at constant voltage: 80 V for $2^1/_2$–3 h. A longer running time of 4 h was used for the DNA sizing experiments. Eight to ten micrograms per milliliter of ethidium bromide in the above Tris buffer was used for overnight staining of the gels. Pictures were taken with a Polaroid Land camera under UV light.

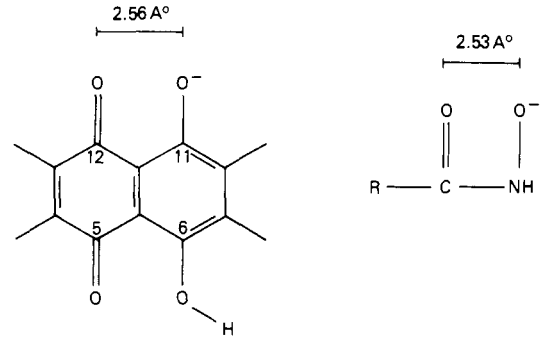

FIGURE 2: Structural similarities of the metal chelation site of adriamycin and acetohydroxamic acid. The anthracycline is on the left and acetohydroxamic acid on the right.

Phenol Extraction. A number of techniques were tried in order to obtain efficient extraction of the adriamycin–iron complex from DNA. Dialysis was ineffective, and extraction with 2-propanol was not adequate. Cold phenol removed the complex from the DNA; however, the recovery of adriamycin with each extraction was quite low, and complete removal of the drug required multiple extractions. On the other hand, we have found phenol extraction at 60 °C very effective, with two extractions giving greater than 97% recovery of the drug–metal complex from DNA. Furthermore, as long as the samples were kept in the dark and did not contain hydrogen peroxide, hot phenol extraction did not result in any DNA fragmentation. The final technique used is summarized below.

Two hundred microliters of 60 °C water-saturated phenol was added to 200 μL of the above test mixture in Eppendorf microtubes with snap tops. This was gently shaken at 60 °C for 1 min, inverting several times. After spinning at 2000 rpm for 4 min, the supernatant containing the DNA was removed to another tube and a second 200 μL of 60 °C phenol added and again extracted at 60 °C for 1 min. After spinning for an additional 4 min, the supernatant was removed and placed in another tube, ready for gel application. Sixteen microliters of each extracted DNA (approximately 0.53 μg) was mixed with 16 μL of a 25% Ficoll–0.1% bromphenol blue solution and 4 μL of water. This was vortexed and placed directly in a well in the agarose gel.

Results

In attempting to study the interaction of the adriamycin–Fe(III) complex with DNA, we faced a number of technical difficulties. On the surface it would seem logical to compare the effects of the adriamycin–Fe(III) complex with adriamycin on one hand and Fe(III) on the other. However, at neutral pH, Fe(III) rapidly polymerizes and becomes unavailable for adriamycin chelation (Spiro et al., 1966). In practice, Fe(III) must be chelated in order to be kept stable and to get reproducible results in studies of the kind we will be presenting. In a previous report, we showed that the acetohydroxamic–iron complex (Figure 2) was an effective iron donor to adriamycin and allowed reproducible formation of a stable drug–metal complex (Myers et al., 1982). Presumably this iron donation works due to the high-affinity constants of adriamycin for Fe(III) of 10^{18}, 10^{11}, and $10^{4.4}$ as compared to $10^{11.4}$, $10^{9.68}$, and $10^{7.23}$ for acetohydroxamic acid (May et al., 1980; Brown et al., 1978). A comparison of the structure of the two ligands reveals interesting similarities and differences. As with adriamycin, the Fe(III) is chelated by a bidentate ligand in which the binding occurs between two oxygens with a 2.53–2.56-Å spacing (Wani et al., 1975; Pettit et al., 1975; Neidle & Taylor, 1977; Courseille et al., 1979; Helm et al., 1980). The two chelates differ, however, in that acetohydroxamic acid

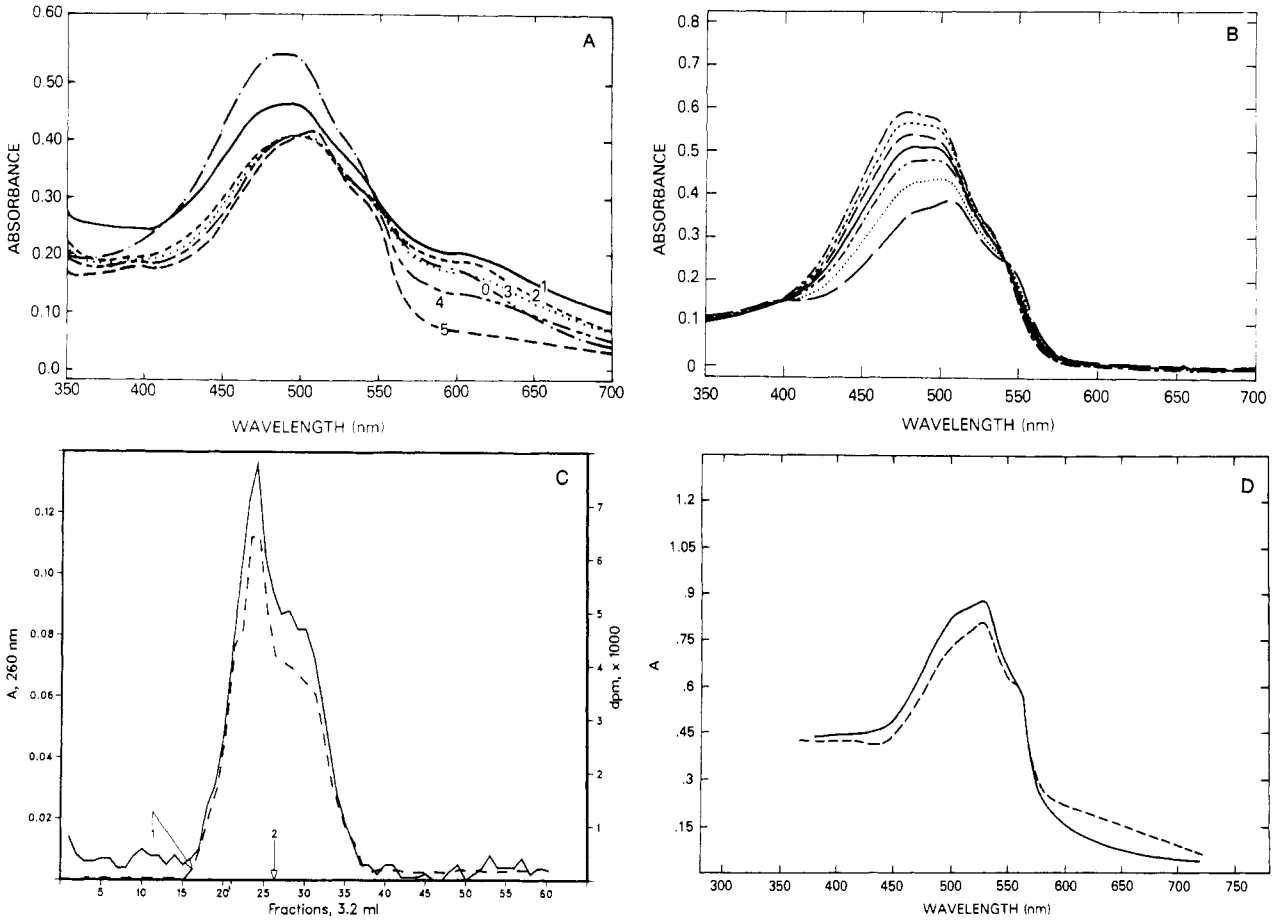

FIGURE 3: Panel A represents the titration of a 25 μM concentration of the adriamycin–Fe(III) complex [25 μM Fe(III) and 50 μM adriamycin], with a range of *E. coli* DNA concentrations: (0) no DNA; (1) 25 μM; (2) 125 μM; (3) 175 μM; (4) 250 μM; (5) 500 μM. All solutions were made in double-distilled water and brought to pH 7.0. Panel B represents the titration of a 50 μM solution of adriamycin with a range of *E. coli* DNA concentrations: (1) (---) no DNA; (2) (- - -) 25 μM; (3) (– –) 50 μM; (4) (—) 125 μM; (5) (–·–·–) 175 μM; (6) (···) 250 μM; (7) (— —) 500 μM. Both adriamycin and DNA were diluted in acetate–barbital buffer, pH 7.0, containing 50 μM EDTA. Panels C and D represent the isolation of the ternary DNA–adriamycin–Fe(III) complex. Comparison of the spectrum of the isolated DNA–adriamycin complex (panel C) compared with that of the ternary DNA–adriamycin–Fe(III) complex (panel D). The reaction mixture for the DNA–adriamycin complex preparation was 100 μM adriamycin and 500 μM *E. coli* DNA, and that for the ternary DNA complex preparation was 200 μM adriamycin, 100 μM ^{59}Fe(III), and 1.0 mM *E. coli* DNA. The reaction was carried out in double-distilled water brought to pH 7.0 with NaOH. These were incubated $^1/_2$ h at room temperature. Two mililiters (76278 cpm) was placed on a 2.6 × 34 cm Sephadex G-50 column at 4 °C and shielded from light. All solutions were made, and the elution was carried in double-distilled water, pH 7.0. Fractions of 3.2 mL were collected and radioactivity and absorbance at both 260 and 505 nm recorded. In panel C, the first arrow marks the void volume and the second arrow, the point of peak absorption at 505 nm. Fractions containing maximum radioactivity and absorbance at 505 nm, which coincided with maximum OD 260 readings, were pooled and lyophilized. The lyophilized complexes were then reconstituted in 1 mL of DDW and the spectra measured [panel D: adriamycin–DNA (—); adriamycin–Fe–DNA (---)].

does not possess the planar chromophore and amino sugar which endow adriamycin with such a rich biochemistry. In addition, acetohydroxamic acid is devoid of the structural features required for DNA intercalation. For these reasons, we have used the acetohydroxamic acid–Fe(III) chelate for two purposes: (1) as an iron donor for adriamycin and (2) as a nonintercalating iron chelate to help us determine what aspect of the adriamycin–iron complex behavior was the general property of Fe(III) chelates rather than a specific property of adriamycin.

Binding of the Adriamycin–Fe(III) Complex to DNA. The ability of adriamycin to bind to DNA via intercalation is both well-known and extensively studied. When preformed adriamycin–Fe(III) complex was added to DNA in concentrations of drug and DNA previously used in the study of adriamycin intercalation (0.1 mM DNA and 0.1 mM adriamycin), a deep purple precipitate formed (Spinelli & Dabrowiak, 1982; Fritzsche et al., 1982). While this behavior indicated association of the drug–metal complex with DNA, it made detailed study of this phenomenon difficult. We next performed a titration of 25 μM adriamycin–iron complex with a range of DNA concentrations. The results of such a titration differ markedly from those obtained with adriamycin (Figure 3A,B). The most distinctive aspect of the titration of the drug–metal complex by DNA is that the charge-transfer band extending out to 600 nm characteristic of the complex undergoes a series of changes depending upon the DNA base pair/metal complex ratio (Figure 3A). At low metal complex/DNA base pair ratios, the charge-transfer band increases in intensity and extends to longer wavelengths. At higher metal complex/DNA base pair ratios, this process reverses itself, and the charge-transfer band declines in intensity and extent as DNA concentrations increase. This decline in absorption at 600 nm correlated with the development of a fine purple precipitate. Initially, however, no such aggregation was noted at the metal complex/DNA ratio of 1/1, and neutral sucrose density gradients done after 1 h showed no aggregation. For this reason, the stability of this solution was followed for 12 h. Over the first 8 h, the absorption at 590 nm gradually declined from 0.27 to 0.20, after which no further change was noted. A question remained over the state of the drug–metal complex remaining in this solution. We had earlier observed that

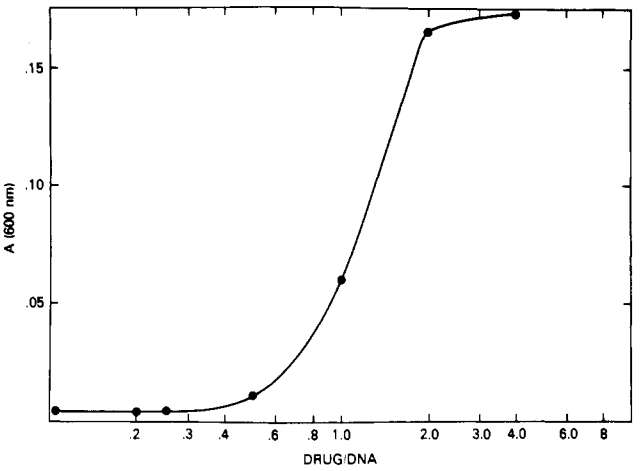

FIGURE 4: Effect of preincubation of adriamycin with *E. coli* DNA upon the subsequent availability of adriamycin for iron binding. Adriamycin (40 μM) was incubated with 10, 20, 40, 80, 200, and 400 μM DNA in acetate–barbital buffer, pH 7.3. After a 30-min incubation, 20 μM Fe(III) in the form of acetohydroxamic acid complex (see Materials and Methods) was added to each dilution and the increase in absorbance at 600 nm measured.

EDTA effectively competes with adriamycin for Fe(III). For this reason, after 12 h the above solution was made 30 μM with respect to EDTA. Over the 10 h, the absorption at 590 nm slowly declined from 0.20 to 0.18. This is in marked contrast to the behavior of the free adriamycin–Fe(III) complex which completely diassociates in less than 30 min in the presence of 30 μM EDTA. Thus incubation of the complex in the presence of DNA leads to the development of a more stable species still able to absorb at 600 nm.

These above results suggested that the adriamycin–Fe(III) chelate may form a ternary complex with DNA which is quite stable and spectrally distinct from both the free adriamycin–Fe(III) complex and DNA-intercalated adriamycin. In order to examine this possibility in more detail, we attempted to isolate the putative drug–metal–DNA complex directly. Both adriamycin and the adriamycin–iron complex are retarded on Sephadex G-50, while DNA elutes near the void volume. When the putative ternary complex was applied to the Sephadex G-50 column, the DNA, iron, and adriamycin eluted together near the void volume of the column (Figure 3C). In this experiment, 91% of the complex was recovered in the DNA-containing fractions. An experiment was performed with DNA and adriamycin alone, and in this case also the adriamycin eluted in the DNA-containing fractions. The DNA-containing fractions from each experiment were pooled separately, lyophilized to dryness, and reconsistituted in a small volume, and the spectrum of each was measured (Figure 3D). These results confirm the existence of a spectrally distinct ternary complex. In a separate experiment (not shown), we found DNA treated with ^{59}Fe–acetohydroxamate bound the radioactive iron well enough that over 90% of the radioactivity was recovered in the DNA fractions. We were unable to detect binding of the acetohydroxamic acid ligand because there was no spectral change which could be used to indicate binding, and radiolabeled acetohydroxamic acid was not available. Thus, we cannot determine whether this chelate donates iron to DNA or binds to it as a unit.

These results do not serve to distinguish whether the adriamycin–iron ternary complex represents DNA-intercalated drug with iron attached or whether another mode of binding is involved. In order to approach this problem, we preincubated a range of DNA concentrations with a constant amount of adriamycin so as to allow intercalation to occur and then added Fe(III). The results, shown in Figure 4, indicated that the charge-transfer band associated with iron binding did not occur until drug/DNA ratios reached 0.5 (two base pairs per drug). Since it is known that intercalated adriamycin occupies a binding site spanning approximately three base pairs (Chaires et al., 1982), these results suggest the only adriamycin available for iron binding was drug not fully involved in intercalation.

Table I: Effect of DNA Addition on the Thiol-Dependent Oxygen Consumption Catalyzed by the Adriamycin–Iron Complex[a]

[DNA] (μM)	DNA/ complex	O_2 consumption (nmol mL^{-1} min^{-1})	control (%)
0		27.1	100
12.5	1	24.8	91.6
25	2	26.9	99.2
50	4	25.3	93.0
100	8	21.5	79.4
200	16	10.4	38.2
499	32	7.7	28.2

[a] The concentrations used were the following: Fe(III), 12.5 μM; adriamycin, 25 μM; glutathione, 20 mM. The reaction was run in acetate–barbital buffer, 20 mM, pH 7.3. The order of addition was buffer, DNA, glutathione, and then drug–metal complex.

Oxygen Consumption by DNA-Bound Complex. DNA-intercalated adriamycin cannot be reduced and cannot undergo the redox cycling that allows the free drug to support the generation of superoxide and hydrogen peroxide (Lown et al., 1977). The fact that intercalated drug cannot be polarographically reduced has been used to measure and compare DNA intercalation by a range of anthracyclines (Berg et al., 1982). However, the adriamycin–iron complex can catalyze nonenzymatic reduction of oxygen by thiols such as glutathione via a reaction which appears to be distinct from the redox cycling discussed above. In addition, the mode of the binding of the drug–metal ion complex to DNA appears to differ appreciably from that of adriamycin. Thus, it was of interest to examine the capacity of DNA to quench thiol-dependent oxygen consumption catalyzed by the drug–metal complex. The results (Table I) show that the DNA-bound drug–metal complex still supports oxygen consumption at nearly its full rate until DNA is added in considerable molar excess. As discussed earlier, concentrations of DNA and the drug–metal complex of this magnitude are associated with some aggregation, which might be expected to effect the reaction between thiol, oxygen, and the DNA-bound complex.

The results of the studies up to this point indicate that the adriamycin–iron complex binds to DNA via a mechanism which can be distinguished from intercalation both on spectral grounds and by the ability of the DNA-bound drug–metal ion complex to catalyze thiol-dependent oxygen reduction.

Catalysis of Thiol-Dependent DNA Cleavage by the Adriamycin–Fe(III) Complex. The fact that DNA-bound adriamycin–Fe(III) complex preserved the ability to catalyze the reduction of oxygen by glutathione suggests that this metal ion complex might also be capable of also causing oxidative destruction of DNA.

Figure 5 illustrates the effect of thiol addition on DNA fragmentation in the presence of adriamycin, the acetohydroxamic acid–Fe(III) complex, or the adriamycin–Fe(III) complex. It is apparent that the adriamycin–iron complex in the presence of glutathione causes extensive DNA fragmentation, while adriamycin, itself did not exhibit activity. The acetohydroxamic acid–ferric ion complex also caused DNA fragmentation, albeit to a lesser degree than did the adria-

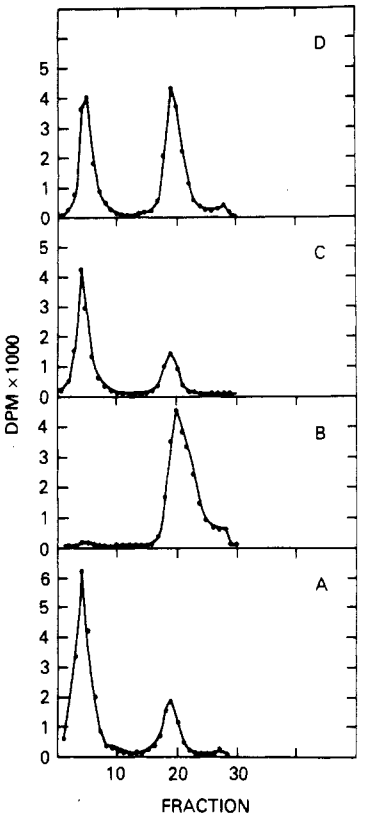

FIGURE 5: Effect of the addition of reduced glutathione to SV-40 DNA plus adriamycin, adriamycin–Fe(III) complex, or the acetohydroxamic acid–Fe(III) complex. The reduced glutathione was diluted in double-distilled water and brought to pH 7.0. All gradients contained 9 μM SV-40 DNA and the following: (A) no additions; (B) 0.25 mM GSH, 50 μM Fe(III), 150 μM acetohydroxamic acid, and 100 μM adriamycin; (C) 0.25 mM GSH and 100 μM adriamycin; or (D) 0.25 mM GSH, 50 μM Fe(III), and 150 μM acetohydroxamic acid.

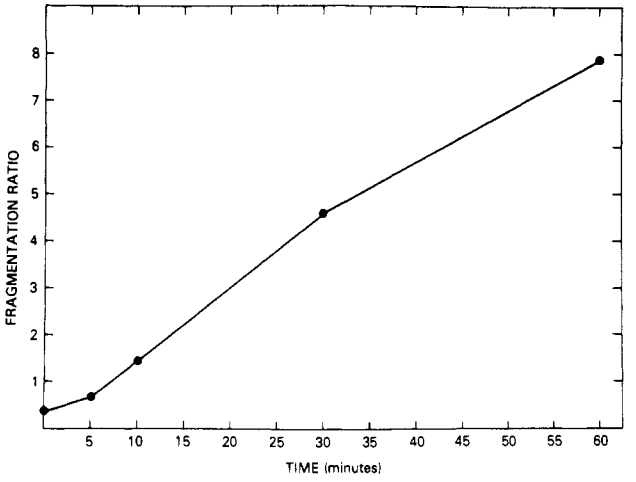

FIGURE 6: Time course of the cleavage of SV-40 DNA in the presence of the adriamycin–Fe(III) complex plus glutathione. The standard reaction mixture for the gradients (as under Materials and Methods) was incubated for varying times, and the resulting fragmentation ratios were plotted.

mycin–iron complex. In our studies, we have found that with acetohydroxamic acid–Fe(III) concentrations of 10 μM, no damage was observed, whereas at this same concentration, the adriamycin–metal ion complex still caused maximal damage.

As part of these studies, we also assessed the time course of the fragmentation reaction caused by the adriamycin–iron complex. As can be seen in Figure 6, after an initial lag period, the damage proceeded in a linear fashion for 30 min, after which the rate gradually declined. In most of the studies which

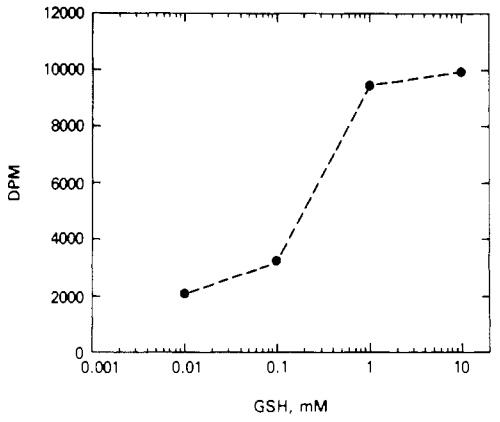

FIGURE 7: DNA fragmentation as a function of glutathione concentration. Fe(III) (25 μM) and adriamycin (50 μM) were incubated with 9 μM ^{3}H SV-40 DNA and the glutathione concentrations shown. Alkaline sucrose gradients were run, and total dpm values in the peaks containing fragmented DNA were compared.

Table II: Effect of Various Inhibitors on the Thiol-Dependent DNA Fragmentation Reaction Catalyzed by the Adriamycin-Fe(III) Complex

inhibitor[a]	% of control fragmentation[b]
superoxide dismutase	165
catalase	35
Me_2SO	75
mannitol	87
histidine	46

[a] The inhibitors were added as indicated to the standard reaction mixture for the alkaline sucrose gradients. The concentrations of each were the following: superoxide dismutase, 120 units/mL; catalase, 400 units/mL; Me_2SO, 0.5 M; mannitol, 5.5 mM; histidine, 10.9 mM. [b] The extent of DNA fragmentation was determined via alkaline sucrose density gradient analysis. The DNA fragmentation was determined for the standard reaction mixture after a 2-h incubation. Parallel incubations were done with the additions specified, and the result was expressed as a percent of the damage seen in the standard reaction mixture.

follow, we have used a 2-h reaction time to allow the DNA fragmentation to go to completion.

Glutathione concentrations in vivo are constrained within a narrow range, and it is, therefore, important to know whether this reaction occurs at biologically relevant glutathione levels. For this reason, the DNA fragmentation reaction was studied over a range of glutathione concentrations. The results (Figure 7) showed a sharp increase in DNA fragmentation between 0.1 and 1.0 mM glutathione as assayed in the alkaline sucrose density gradients.

The alkaline sucrose density gradient, while a valuable tool for studies of this type, detects both frank DNA breaks and alkaline labile regions. The phenol extraction–neutral agarose gel technique we developed earlier offers a method capable of detecting DNA fragmentation in the absence of exposure to alkaline pH. For this reason, we have repeated the glutathione titration above using 1% neutral agarose gels to follow the fragmentation of the DNA. With this technique, the DNA damage increased more gradually over glutathione concentrations from 0.1 to 10 mM (data not shown). In both cases, however, DNA fragmentation was extensive in the physiologic glutathione concentration range 5–20 mM.

Effect of Inhibitors on the Thiol-Catalyzed Fragmentation of DNA. Previous studies had shown that the adriamycin–Fe(III) complex catalyzed the GSH-dependent production of superoxide and hydrogen peroxide (Myers et al., 1982). For this reason, we next examined the role of these substances in

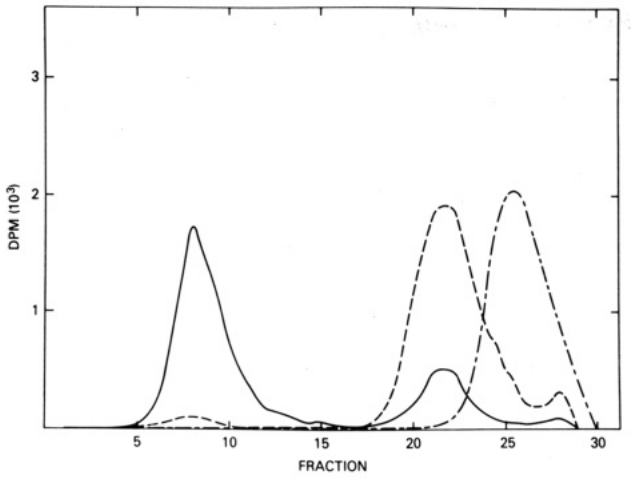

FIGURE 8: DNA fragmentation as a function of hydrogen peroxide concentration (determined by alkaline sucrose gradient): 10 μM SV-40 DNA, and the complex of 100 μM adriamycin and 50 μM Fe(III), treated with (---) 0.5 μM H_2O_2 and (-·-) 50 μM H_2O_2; (—) control of 10 μM DNA treated with 100 μM H_2O_2.

the glutathione-catalyzed cleavage of DNA. In the alkaline sucrose density gradient, we found that catalase caused nearly complete inhibition of DNA damage, while hydroxyl radical scavengers such as mannitol, histidine, and Me_2SO caused partial inhibition only in high concentrations (Table II). Surprisingly, superoxide dismutase measurably increased the DNA damage. A parallel experiment done by using the neutral agarose gel technique confirmed the above results with the exception that superoxide dismutase appeared to cause partial protection. Because of the discrepancy in the results given by the two techniques used, the role of superoxide remains unclear. Nevertheless, these results suggest that the generation of hydrogen peroxide plays a central role in the thiol-stimulated DNA fragmentation reaction.

Catalysis of Hydrogen Peroxide Dependent DNA Damage by the Adriamycin–Iron Complex. Because the experiments with thiol catalysis of DNA destruction by the adriamycin–iron complex pointed to a central role for hydrogen peroxide, we next looked at the reaction of hydrogen peroxide with DNA in the presence and absence of the adriamycin–iron complex. Figure 8 shows that while 0.1 mM H_2O_2 itself caused no damage, 0.5 μM H_2O_2 plus the drug–metal ion complex caused nearly complete disappearance of the intact DNA peak. At higher hydrogen peroxide concentrations, additional fragmentation was observed. This process reached saturation at 50 μM, at which point the DNA sedimented near the top of the gradient (Figure 8).

The concentration dependence of this reaction was also studied by using the phenol extraction–neutral agarose gels with results which confirmed those obtained with the alkaline sucrose density gradients.

Many iron chelates are capable of catalyzing oxidation of organic compounds by hydrogen peroxide (Aust & Svingen, 1982). Earlier we had shown that the iron in ferric acetohydroxamate also binds to DNA. The question thus arises as to the specificity of this hydrogen peroxide dependent DNA cleavage reaction. In order to evaluate this in more detail, we studied the effect of a range of acetohydroxamic acid–iron or adriamycin–iron concentrations on the hydrogen peroxide dependent DNA cleavage reaction. The results (Figure 9B) show acetohydroxamic acid–Fe(III) can catalyze DNA cleavage by hydrogen peroxide. The fragmentation pattern was very intesting in that it revealed formation of form II DNA and an additional fairly well-defined fragment peak

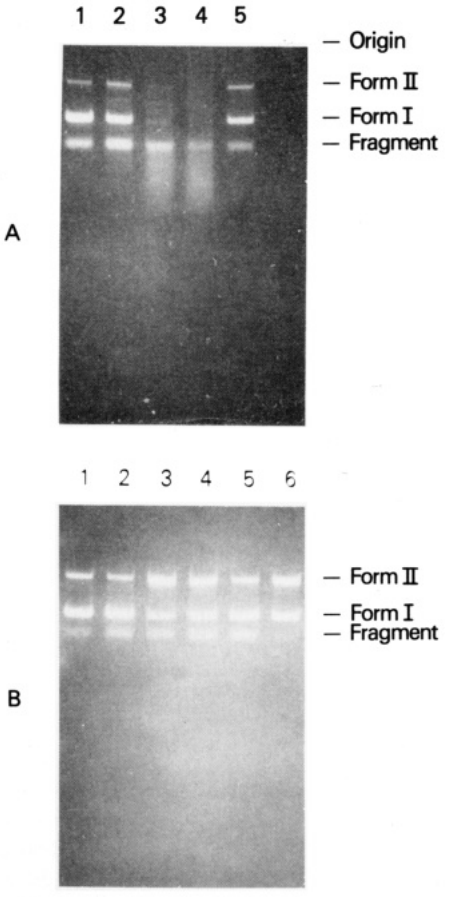

FIGURE 9: Hydrogen peroxide dependent DNA cleavage caused by the adriamycin–iron complex as compared with that by the acetohydroxamic acid–iron complex. All gels were extracted twice with 60 °C H_2O-saturated phenol. Each well contained 100 μM SV-40 DNA, with the following additions. Panel A: (1) 5 μM Fe(III), 10 μM adriamycin, and 50 μM H_2O_2; (2) 10 μM Fe(III), 20 μM adriamycin, and 50 μM H_2O_2; (3) 50 μM Fe(III), 100 μM adriamycin, and 50 μM H_2O_2; (4) 100 μM Fe(III), 200 μM adriamycin, and 50 μM H_2O_2; (5) 100 μM Fe(III), 200 μM adriamycin, and 0 μM H_2O_2. Panel B: (1) 50 μM Fe(III), 150 μM acetohydroxamic acid, and 50 μM H_2O_2; (2) 100 μM Fe(III), 300 μM acetohydroxamic acid, and 50 μM H_2O_2; (3) 500 μM Fe(III), 1.5 mM acetohydroxamic acid, and 50 μM H_2O_2; (4) 1 mM Fe(III), 3 mM acetohydroxamic acid, and 50 μM H_2O_2; (5) 5 mM Fe(III), 15 mM acetohydroxamic acid, and 50 μM H_2O_2; (6) 5 mM Fe(III), 15 mM acetohydroxamic acid, and 0 μM H_2O_2.

migrating more rapidly than supercoiled DNA. Through the use of *Hin*dIII fragments of phage λ and *Hae*III fragments of ϕX174 RF as molecular weight markers, we were able to determine that this fragment peak represented a 2200–2500 base pair fragment. Since the SV-40 DNA genome contains 5600 base pairs, this indicated that the acetohydroxamic acid–Fe(III) complex cuts SV-40 DNA approximately in half. Of course, this conclusion is based on the assumption that the DNA fragment produced has the same charge and shape (linear) as the marker fragments. Additional studies are required to test the validity of this size assignment. Even at very high Fe(III) concentrations, further fragmentation did not occur. While the adriamycin–Fe(III) complex caused a similar fragmentation pattern at much lower concentrations, above 50 μM it caused extensive DNA degradation (Figure 9A). Hydrogen peroxide alone at the concentration used (50 μM) did not cause DNA damage. It is also interesting to note that at 100 μM the drug–metal complex cleaved DNA by itself albeit to a lesser degree than it did in the presence of hydrogen peroxide (Figure 9A, lanes 5 and 6). This DNA cleaving ability of the drug–metal complex was removed by addition

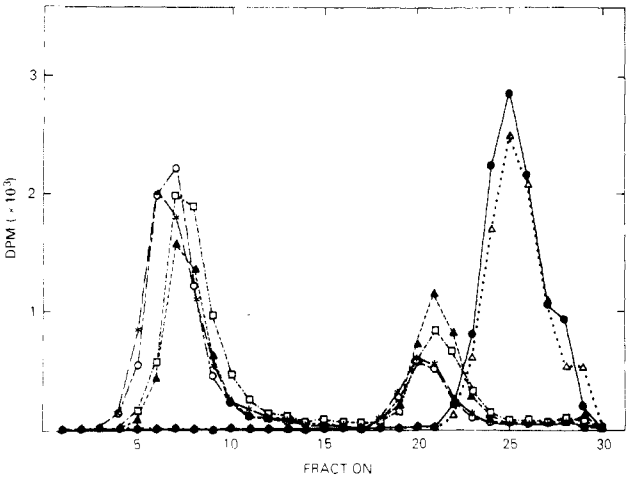

FIGURE 10: Effect of inhibitors on the cleavage of SV-40 DNA in the presence of hydrogen peroxide plus the adriamycin–iron complex as assayed in alkaline sucrose gradients. In addition to 10 μM ^{3}H SV-40 DNA and 100 μM H_2O_2, each reaction mixture was modified in the following way: (●) 100 μM adriamycin and 50 μM Fe(III); (△) 120 units/mL superoxide dismutase, 100 μM adriamycin, and 50 μM Fe(III); (▲) 400 units/mL catalase, 100 μM adriamycin, and 50 μM Fe(III); (asterisk) 120 units/mL superoxide dismutase; (□) 400 units/mL catalase; (○) no additions. Inhibitors were added first and vortexed, followed by the addition of the drug–metal ion complex and then hydrogen peroxide.

of catalase, suggesting that it was due to the presence of trace amounts of H_2O_2. Thus, from these results it is apparent that the adriamycin–Fe(III) complex is much more active than the acetohydroxamic acid–Fe(III) complex in that it both functions at a lower concentration and causes far more extensive DNA degradation.

We next studied the effect of superoxide dismutase, catalase, and hydroxyl radical scavengers in order to gain additional insight as to the mechanism involved in this H_2O_2-dependent DNA cleavage reaction. Again, catalase gave almost complete protection, while superoxide dismutase was without effect (Figure 10). The hydroxyl radical scavengers mannitol, histidine, and Me_2SO gave only partial protection (Figure 10) at the concentrations used. In a separate experiment (not shown), we increased mannitol to 1.4 M and Me_2SO to 1 M and saw increased, although still partial, protection.

Discussion

The present study has documented three salient properties of the adriamycin–iron complex. First, it binds to DNA to form a ternary complex composed of DNA, Fe(III), and adriamycin. This ternary complex appears to be quite stable and to differ in a number of ways from the DNA intercalation characteristics of metal-free adriamycin. Second, the DNA-bound adriamycin–iron complex preserves its ability to catalyze the reduction of oxygen by glutathione to yield hydrogen peroxide. Third, the DNA-bound drug catalyzed the cleavage of DNA by hydrogen peroxide.

DNA Binding. As mentioned in the introduction, it has long been known that the Cu(II)–adriamycin complex will bind to DNA. Recently, Spinelli & Dabrowiak (1982) have studied this in some detail, and their results indicated that the Cu(II) complex binds weakly to DNA. The behavior of the adriamycin–Fe(III) complex differs markedly from this in that the ternary adriamycin–iron–DNA complex shows little dissociation after 10 h in the presence of EDTA and is stable enough to isolate. Furthermore, the adriamycin–iron complex shows considerable tendency to aggregate DNA. While the present study has not defined the nature of the interaction between DNA and the adriamycin–iron complex, the observations do allow some speculation as to the nature of the binding. The most straight forward explanation would be to propose a version of the intercalation geometry described by Quigley et al. (1980) for adriamycin, with some increase in DNA unwinding to accommodate the addition of a bulky metal ion. This would be analogous to that recently proposed for the Cu(II)–adriamycin complex (Fritzsche et al., 1982). This concept is consistent with the hypso- and bathochromic shift seen at high drug/DNA ratios. This type of spectral shift is seen when adriamycin undergoes DNA intercalation (Figure 3B) or a stacking interaction with itself or other planar aromatic systems (Gianni et al., 1983). One major difficulty of this model is that the metal ion would then be buried within the double helix, and in that setting it is difficult to imagine that the metal ion would still preserve its capacity to catalyze the reduction of oxygen by the tripeptide glutathione: steric factors alone would seem to dictate a markedly reduced reaction rate. A second objection to this proposal is that adriamycin interacalation has proved to be very sensitive to substituents on rings B and C. For example, replacement of the phenolic protons on adriamycin at C-6 or C-11 with methyl groups markedly reduces the ability of these drugs to intercalate (Zunino et al., 1981). This decreased affinity is presumed to occur because the greater bulk of the methyl groups as compared with a proton makes intercalation more difficult. By analogy, one would expect the added bulk of a metal ion in the same position to weaken the affinity of the adriamycin for DNA. In this regard, it is interesting to note that while Cu(II)–porphyrin complexes intercalate DNA, the equivalent Fe(III) complexes do not. However, in the present study, the ternary complex proved quite stable, and in fact, rather vigorous conditions were required to disrupt it (phenol extraction at 60 °C). A third objection is that DNA-intercalated adriamycin appears to be unavailable for iron binding. For these reasons, we think that the iron complex is not likely to bind to DNA via intercalation.

An alternate proposal is suggested by the observation, mentioned earlier, that a common histochemical technique for staining DNA depends upon the use of iron to bind a variety of hydroxyquinone dyes to DNA (see Figure 1). This technique has been thought to depend upon the metal ion [usually Fe(III) or Al(III)] binding to DNA on one hand and being chelated by the hydroxyquinone dye on the other hand. The metal thus acts as a bridge between the chromophore and DNA.

On the basis of this concept, one can speculate as to what structural features of adriamycin might explain the stability with which its iron complex binds to DNA. The evidence available (to be published elsewhere) suggests that the Fe(III) binding site of adriamycin is between the oxygens at C-11 and C-12. We have used the X-ray crystal coordinates for related anthracyclines to build a space-filling model of adriamycin with Fe(III) chelated at C-11 and C-12 (Wani et al., 1975; Pettit et al., 1975; Neidle & Taylor, 1977; Courseille et al., 1979). The most interesting structural feature of this model is that 13 Å separate the iron from the sugar amine, which at physiological pH can be expected to bear a positive charge. The phosphate backbone is characterized by a 6.5-Å spacing. Thus, it is possible to envision a structure where the iron binds to one phosphate group, the next phosphate group is not involved in the binding, but that sugar amine binds to the third phosphate. The result is a drug–Fe(III) bridged structure that spans a binding site of three phosphate groups (13 Å) along the DNA backbone. There are several attractive features of

this model. First, Fe(III) has a very high affinity for phosphate with an association constant of greater than 10^{20}. Second, this and interaction of the positively charged sugar amine with the phosphate backbone would be consistent with the observed stability of the ternary complex. Third, this proposal leaves the iron sufficiently exposed so as to allow for the redox catalysis observed. Fourth, this binding mode would explain the ability of the adriamycin–iron to aggregate DNA in that a free iron d orbital is available to bind to a phosphate group on a second adjacent double helix, allowing the formation of aggregates. Thus, this model combines the advantages of a precise geometric fit between the drug–metal ion complex and DNA with a reasonable explanation of most of the results we have observed. However, more specific physicochemical techniques are required to validate this hypothesis.

Thiol Catalysis of DNA Destruction. The reaction by which the adriamycin–iron complex cleaves DNA in the presence of glutathione warrants some discussion. The results of this study suggest a two-stage process. The first step is apparently the thiol-catalyzed production of hydrogen peroxide either directly or via superoxide followed by dismutation of superoxide to yield hydrogen peroxide. The ability of iron chelates to catalyze this thiol-dependent reduction is well-known and will not be discussed further, except to note that in a previous paper, we had demonstrated that both the adriamycin–iron and the acetohydroxamate–iron chelate have this capacity (Myers et al., 1982). In any case, the key aspect of this reaction appears to be the generation of hydrogen peroxide, because addition of catalase effectively prevents DNA damage. The second step appears to be a reaction between hydrogen peroxide, the drug–metal complex, and DNA which leads to DNA damage. The adriamycin–Fe(III) complex proved an extremely efficient catalyst of this hydrogen peroxide dependent DNA cleavage, causing extensive DNA damage at peroxide concentrations more than 3 orders of magnitude below the point where peroxide alone damages DNA. The fact that ferric acetohydroxamate is able to catalyze the same reaction, albeit much less efficiently, suggests that the role of adriamycin in this reaction may be merely to enhance the efficiency of a reaction which is a basic property of ferric ion chelates. On the basis of what is known of Fe(III) chemistry, two distinct reaction pathways have been invoked for reactions of this type (Walling, 1975). These two possibilities involve either formation of a ferryl ion product via an iron peroxo intermediate or hydroxyl radical formation. Formation of hydroxyl radical from Fe(III) plus hydrogen peroxide has, for the most part, been demonstrated under nonphysiologic conditions. In the present study, hydroxyl radical scavengers did lessen DNA damage. However, very high concentrations were required, and for this reason we question the specificity of these probes. We are currently in the process of trying to determine the relative importance of hydroxyl radical vs. ferryl ion formation in the DNA cleavage reaction through the use of more specific methods such as spin trapping.

Recently it has been shown that DNA or nucleotide-bound Fe(II) but not Fe(III) supported peroxide-dependent hydroxyl radical production (Floyd & Lewis, 1983). Similarly, ferryl ion formation is also favored by reduction of Fe(III) to Fe(II) (Chin et al., 1980). For this reason, we found the reaction of hydrogen peroxide with the Fe(III)–adriamycin complex suprising. A third possibility does exists in that adriamycin is a hydroxyquinone theoretically capable of reducing Fe(III) to Fe(II). The Fe(II) thus formed might then react with peroxide via well-established reaction schemes to yield hydroxyl radical or ferryl ion species. At present, however, no data are available to document the actual valence of the drug-bound iron. Finally, H_2O_2 itself can reduce Fe(III) to Fe(II) which can, in turn, react with H_2O_2 to produce either hydroxyl radical or ferryl ion.

Comparison of the Two Modes of Adriamycin-Induced Formation of Reactive Oxygen Species. From the above, it is now apparent that adriamycin has two distinct mechanisms by which it can create reactive oxygen species: the transition metal ion dependent mechanism just discussed or via the well-described reaction between the adriamycin semiquinone and oxygen (Bachur et al., 1977). It is important to contrast the metal chelate dependent mechanism with the consequences of adriamycin semiquinone radical formation. Reduction of adriamycin to the semiquinone in the presence of oxygen is characterized by the production of a range of reactive oxygen species including hydroxyl radical. In the presence of DNA, this leads to DNA cleavage which is lessened by hydroxyl radical scavengers (Lown et al., 1977). However, as mentioned earlier, none of this chemistry is possible with DNA-intercalated drug. Thus, for adriamycin to cause radical-mediated DNA damage, there must be nonintercalated drug available for reduction. The site of adriamycin reduction closest to the DNA is the cytochrome P-450 reductase present on the nuclear envelope (Bachur et al., 1982). DNA damage by this mechanism requires the radical species generated to diffuse from a site of activation such as the nuclear envelope to the DNA target. While the drug semiquinone radical, superoxide, and hydrogen peroxide have sufficient stability for this purpose, it is very unlikely that hydroxyl radical, the species directly responsible for DNA damage in this case, can do so.

In contrast to the above, the DNA-bound adriamycin–iron complex is able to catalyze directly the cleavage of DNA in the presence of trace amounts of hydrogen peroxide. The hydrogen peroxide utilized for this reaction can either be generated locally via the thiol-dependent reduction of oxygen or from more remote sites of hydrogen peroxide generation. Besides the potential advantage in efficiency of local rather than distant generation of reactive species, this mechanism has interesting implications. Adriamycin semiquinone formation and thus superoxide and hydrogen peroxide production can be catalyzed by multiple enzymes including xanthine oxidase, cytochrome P-450 reductase, mitochondrial NADH dehydrogenase, and other flavoprotein reductases. In heart muscle, for example, adriamycin-stimulated superoxide formation can be detected from multiple subcellular organelles (Doroshow, 1983). Thus, adriamycin semiquinone formation can act as a source of hydrogen peroxide to the adriamycin–iron complex. In this sense, the two mechanisms would be expected to operate cooperatively to enhance DNA damage.

While the importance of the adriamycin–iron complex in vivo has not been directly studied, there exists circumstantial evidence that suggests its involvement in drug toxicity. First, Kappus et al. (1980) have reported that coadministration of iron and adriamycin leads to an increase in whole animal toxicity and lipid peroxidation. Second, Herman et al. (1974, 1979) have shown that the EDTA derivative ICRF 159 and the related compound ICRF 187 are extremely effective in preventing adriamycin and daunomycin cardiac toxicity. Recently, ICRF 159 has been shown to hydrolyze intracellular to *N*,*N*′-bis(carboxamidomethyl)-*N*,*N*′-bis(carboxymethyl)-1,2-diaminopropane, which is a powerful chelator of transition metal ions (Huang et al., 1982). Furthermore, these compounds have been shown to cause an increase in the urinary secretion of a range of transition metal ions (Witting et al., 1979). Thus, one explanation for the cardioprotective effect

of the ICRF compounds would be their ability to prevent the formation of adriamycin–transition metal chelates.

While the above results are suggestive, it would be desirable to have a more direct test of the formation and action of the adriamycin–iron complex in vivo. Perhaps the demonstration, in the present study, that the adriamycin–iron chelate forms a stable ternary complex with DNA will aid in this process.

Acknowledgments

We thank Dr. Brian Corden and Dr. Kenneth Cowan for their helpful discussions and Sharon Ray and Claire Rosenblum for their editorial assistance.

References

Aust, S. D., & Svingen, B. A. (1982) *Free Radicals Biol. 5*, 1.

Bachur, N. R., Gordon, S. L., & Gee, M. L. (1977) *Mol. Pharmacol. 13*, 901.

Bachur, N. R., Gee, M. V., & Friedman, R. D. (1982) *Cancer Res. 42*, 1078.

Berg, H., Horn, G., & Luthardt, V. (1982) *Bioelectrochem. Bioenerg. 8*, 537.

Brown, D. A., Chidambaram, M. V., Clarke, J. J., & McAllese, D. M. (1978) *Bioinorg. Chem. 9*, 255.

Calendi, E., DiMarco, A., Reggiani, M., Scarpinato, B., & Valentini, L. (1965) *Biochim. Biophys. Acta 103*, 25.

Chaires, J. B., Dattagupta, N., & Crothers, D. M. (1982) *Biochemistry 21*, 3933.

Chin, D. H., LaMar, G. N., & Balch, A. L. (1980) *J. Am. Chem. Soc. 102*, 5947.

Courseille, C., Busetta, B., Geofre, S., & Hospital, M. (1979) *Acta Crystallogr., Sect. B B35*, 746.

Doroshow, J. H. (1983) *Cancer Res. 43*, 460.

Fishman, M. M., & Scwartz, I. (1974) *Biochem. Pharmacol. 23*, 2174.

Floyd, R. A., & Lewis, C. A. (1983) *Biochemistry 22*, 2545.

Fritzsche, H., Triebel, H., Chaires, J. B., Dattagupta, W., & Crothers, D. M. (1982) *Biochemistry 21*, 3940.

Helm, D. V. D., Baker, J. R., Eng-Wilmont, D. L., Hossain, M. B., & Loghry, R. A. (1980) *J. Am. Chem. Soc. 102*, 4224.

Herman, E., Botray, R., & Chadwick, D. M. (1974) *Toxicol. Appl. Pharmacol. 27*, 517.

Herman, E., Ardalan, B., Rier, C., Waravdekar, V., & Krof, S. (1979) *Cancer Treat. Rep. 63*, 89.

Huang, Z. X., May, P. M., Quinlan, K. M., Williams, D. R., & Creighton, A. M. (1982) *Agents Actions 12*, 4.

Kappus, H., Muliawan, H., & Scheulen, M. E. (1980) in *Mechanisms of Toxicity and Hazard Evaluation* (Holmstedt, B., Lauwerys, R., Mercier, M., & Roberfroid, M., Eds.) p 635, Elsevier/North-Holland Biomedical Press, New York.

Lillie, R. D., & Fallmer, H. M. (1976) in *Histopathologic Technic and Practical Histochemistry*, 4th ed., p 123, McGraw-Hill, New York.

Lown, J. W., Sim, S. K., Majumdar, K. C., & Chang, R. Y. (1977) *Biochem. Biophys. Res. Commun. 76, 705.*

May, P. M., Williams, G. N., & Williams, D. R. (1980) *Inorg. Chim. Acta 46*, 221.

Midelens, P., & Levinson, W. (1978) *Bioinorg. Chem. 9*, 441.

Myers, C. E., Gianni, L., Simone, C. B., Klecker, R., & Green, R. (1982) *Biochemistry 21*, 1707.

Neidle, S., & Taylor, G. (1977) *Biochim. Biophys. Acta 479*, 450.

Pasternak, P. F., Gibbs, E. G., & Villafranca, J. J. (1983) *Biochemistry 22*, 2406.

Pettit, G. R., Eirek, J. J., Herold, C. L., Ode, R. H., Von Dreele, R. B., Brown, P., Brahnikora, M. G., & Granse, G. F. (1975) *J. Am. Chem. Soc. 97*, 7387.

Phillips, D. R., & Carlyle, G. (1981) *Biochem. Pharmacol. 30*, 2021.

Quigley, G. J., Wang, A. H. J., Ughetto, G., Van Der Marel, G., Van Boom, J. H., & Rich, A. (1980) *Proc. Natl. Acad. Sci. U.S.A. 77*, 7204.

Rusconi, A. (1966) *Biochim. Biophys. Acta 123*, 627.

Someya, A., & Tanaka, N. (1979) *J. Antibiot. 32*, 839.

Spinelli, M., & Dabrowiak, J. L. (1982) *Biochemistry 21*, 5862.

Spiro, T. G., Allerton, F. E., Renner, J., Tergis, P., Bils, R., & Sallsman, P. (1966) *J. Am. Chem. Soc. 88*, 12.

Sugioka, K., Nakano, H., Noguchi, R., Tsuchiya, J., & Nakano, M. (1981) *Biochem. Biophys. Res. Commun. 100*, 1251.

Walling, C. (1975) *Acc. Chem. Res. 8*, 125.

Wani, M. C., Taylor, M. E., Wall, A. T., McPhail, A. T., & Onan, K. A. (1975) *J. Am. Chem. Soc. 97*, 5955.

Witting, V., Bertram, H. P., Schumacher, E., & Ritter, G. (1979) *Int. Arch. Occup. Environ. Health 42*, 365.

Zunino, F., Casazza, A., Pratesi, G., Formelli, F., & DiMarco, A. (1981) *Biochem. Pharmacol. 30*, 1856.